## W. H. PITTS, III

P.O. Box 15946,
Nashville, Tenn.;
Presently, Department of Mechanical
Engineering, Vanderbilt University,
Nashville, Tenn. 37215

## C. F. DEWEY, Jr.

Department of Mechanical Engineering,
Massachusetts Institute of Technology,
Cambridge, Mass. 02139

# Spectral and Temporal Characteristics of Post-Stenotic Turbulent Wall Pressure Fluctuations

*The power spectral density of turbulent wall pressure fluctuations was measured in a tube downstream of a model arterial constriction. The flow parameters were varied from steady flow to conditions simulating human arterial pulsatile flow. Within the experimental uncertainty ($\pm 10$ percent in characteristic turbulent frequency, $f_o$, and $\pm 25$ percent in absolute rms pressure fluctuation amplitude), turbulent flow at the peak of systole produces wall pressure fluctuations identical to those of a steady flow at the same Reynolds number.*

## Introduction

Flow in the major human arteries is characterized by a large unsteady component; typically the ratio, $\beta$, of mean flow to peak flow is 1/4. For many years there has been continuing controversy regarding the relationship between flow properties measured in steady-state in-vitro experiments and the flow properties which would exist under pulsatile flow conditions simulating human arterial pulsatile waveforms. It is the objective of this paper to examine the turbulence produced by pulsatile flow through a simulated arterial lesion and to compare our results with similar data obtained in steady flow.

It is known that a severe arterial lesion will produce flow separation near the point of minimum cross-sectional area and, at the Reynolds numbers characteristic of human systolic peak flow, turbulence distal to the constriction. Regions of flow separation and unsteady flow have been associated by numerous authors with exacerbated arterial disease (e.g., Fox and Hugh [1], Duguid [2], Gutstein, et al. [3], Fry [4], Caro, et al. [5], Stehbens [6] and the references therein). Additional clinical motivation for the study of post-stenosis turbulence arises from the fact that the intra-arterial wall pressure fluctuations produce disturbances detectable at the body surface near the lesion, and these disturbances may be analyzed to yield an estimate of the residual lumen diameter (Lees and Dewey [7], Fredberg [8], Duncan, et al. [9]). This analytical method, called phono-angiography, relates the residual lumen diameter, $d$, to the

characteristic frequency, $f_o$, of the power spectral density of the wall pressure fluctuations and the post-stenosis volumetric mean velocity, $U$.

Numerous investigations have been conducted which elucidate the basic features of the flows produced by stenosislike geometries. Among the most complete in-vitro experiments are those of Johansen [10], Young and colleagues [11–13], Reul, et al. [14], Back and Roschke [15, 16], Logan [17], Yellin [18], Fredberg [19], Tobin, et al. [20], and Clark [21]. Theoretical studies of such geometries, which are particularly relevant to laminar flow downstream of the constriction, include those of Macagno and Hung [22], Cheng, et al. [23], and Daly [24].

Much less information is available on the spectral character of the turbulent fluctuations under these conditions. Fricke [25] measured the rms pressure fluctuation level and power spectral density of the wall pressure fluctuations downstream of a two-dimensional step in uniform steady flow. Turbulent spectra were obtained by Yellin [26] and Kim and Corcoran [27] with microphones placed in the flow distal to a constriction. These two experiments were performed with steady flow in-vitro models. Both steady flows and pulsatile flows through orifices were investigated by Clark [21]. His extensive measurements relate to turbulent velocity fluctuations in the central region of flow. A similar experiment was performed by Sacks, Tickner, and Macdonald [28] by inserting orifices in the descending aortas of living dogs; unfortunately, only qualitative spectra were obtained.

Fredberg [19] performed a comprehensive series of steady-flow experiments in which the power spectral density, rms magnitude, and axial distribution of wall pressure fluctuations were measured distal to model arterial constrictions. He demon-

strated that, at Reynolds numbers[1] $(u_j d/\nu)$ characteristic of clinically significant arterial disease, the power spectral density was constant at low frequencies and then, beyond a clearly defined characteristic "break frequency," $f_o$, decreased as $(f/f_o)^{-10/3}$. Other details of his findings will be examined in later sections; we wish to point out here, however, that the slope of the power spectral density found by Fredberg [19] in steady flow is consistent with the clinical findings of Gruber [29] and Duncal, et al. [9] at peak systole when appropriate account is taken of the spectrally selective transmission of wall pressure fluctuations to the surface of the skin [8].

In all of the investigations cited in the previous paragraphs, use has been made, either explicitly or implicitly, of the assumption that flow through a stenosed human artery at the peak of systole is identical in all essential respects to a steady flow through the same geometrical configuration at the same Reynolds number. This point of view can be justified qualitatively by recognizing that: (a) the sharp contraction on the proximal (upstream) side of the occlusion effectively minimizes, at the point of minimum cross-sectional area, any velocity profile differences which would arise from unsteady effects; and (b) near the peak of systole, when the velocity is a maximum and changing slowly, the turbulence distal to the constriction is established rapidly compared to the time required for the velocity to change by an appreciable amount.

We report here a systematic investigation of wall pressure fluctuations distal to a simulated arterial constriction as a function of: the nondimensional magnitude of velocity modulation, $\beta \equiv U_{\text{mean}}/U_{\text{peak}}$; the nondimensional frequency of modulation (Womersley number), $\alpha \equiv D(\omega/4\nu)$; and Reynolds number, $\text{Re} \equiv UD/\nu$. The experimental results are presented in terms of two nondimensional parameters, $\Pi_1$ and $\Pi_2$, which relate the characteristic unsteady acceleration forces in the fluid to the convective acceleration forces and viscous forces acting on the fluid. $\Pi_1$ and $\Pi_2$, are simply appropriate combinations of the nondimensional parameters $\alpha$, $\beta$, and Re.

## Experimental Methods

The test apparatus, described in detail elsewhere [30], is a servo-controlled hydraulic system which is electrically programmable to deliver flow pulses matching most combinations of the following parameters: Reynolds number $(UD/\nu) \equiv \text{Re} = 0$ to $10^4$; Womersley parameter $[D(\omega/4\nu)^{1/2}] \equiv \alpha = 1.8$ to $18$; depth of velocity modulation $(U_{\text{mean}}/U_{\text{peak}}) \equiv \beta = 0.06$ to $1$; and containing harmonic waveform components up to the



Fig. 1   Schematic diagram of pulsatile flow system (from Pitts and Dewey (1975))



'O' RING SEAL

Fig. 2   Cross section of the stenosis geometry

8th harmonic of the fundamental period. The actual flow velocity in the simulated artery has been observed to follow the programmed electrical command signal with excellent precision and reproducibility. Silicon oil with a viscosity of 100 centipoise was used as a test fluid. Flow velocities were measured using a Carolina Medical Electronics Model 331 electromagnetic flowmeter, with a frequency response flat from 0–50 Hz. Fig. 1 is a block diagram of the system.

The test section in which wall pressure fluctuation measurements were made was originally used by Fredberg [19]. The constriction was axially symmetric, exhibiting a circular arc

---

[1] Here $u_j$ is the volumetric mean velocity at maximum constriction, $d$ is the diameter of the occluded lumen, and $\nu$ is the kinematic viscosity.

---

## Nomenclature[1]

$A$ = area ratio, $D^2/d^2$

$d$ = minimum tube diameter at constriction

$d_t$ = diameter of the active sensing area of the transducer

$D$ = diameter of tube distal to constriction

$f_o$ = spectral break frequency (see Fig. 4)

$f$ = frequency

$H$ = distance from tube center to surface (see Fig. 10)

$l$ = axial distance from minimum cross section to point of jet reattachment

$L$ = distance from minimum section

to point of maximum wall pressure fluctuation intensity

$R$ = tube radius, $D/2$

$\text{Re}$ = $UD/\nu$

$\text{Re}_j$ = $u_j d/\nu$

$t$ = time

$u_j$ = jet velocity

$u_{\text{peak}}$ = peak value of jet velocity during cycle

$U$ = area-weighted mean velocity in tube section distal to constriction

$U_{\text{mean}}$ = time mean value of $U$

$U_{\text{peak}}$ = peak value of $U$ during cycle

$x$ = distance from minimum section to point of measurement

$\alpha$ = $D(\omega/4\nu)^{1/2}$

$\beta$ = $(U_{\text{mean}}/U_{\text{peak}})$

$\gamma$ = $\tau_p/\tau_H$

$\mu$ = viscosity of fluid

$\nu$ = kinematic viscosity of fluid $(\mu/\rho)$

$\Pi_1$ = $[\beta(1-\beta)/A\gamma]$ $[l/U_{\text{mean}}\tau_H]$

$\Pi_2$ = $[2(1-\beta)\alpha^2/A\pi\gamma]$

$\rho$ = fluid density

$\tau_H$ = time between waveform cycles (see Fig. 3)

$\tau_P$ = rise time of systolic waveform (see Fig. 3)

$\tau_W$ = time width of analysis segment of data (see Fig. 3)

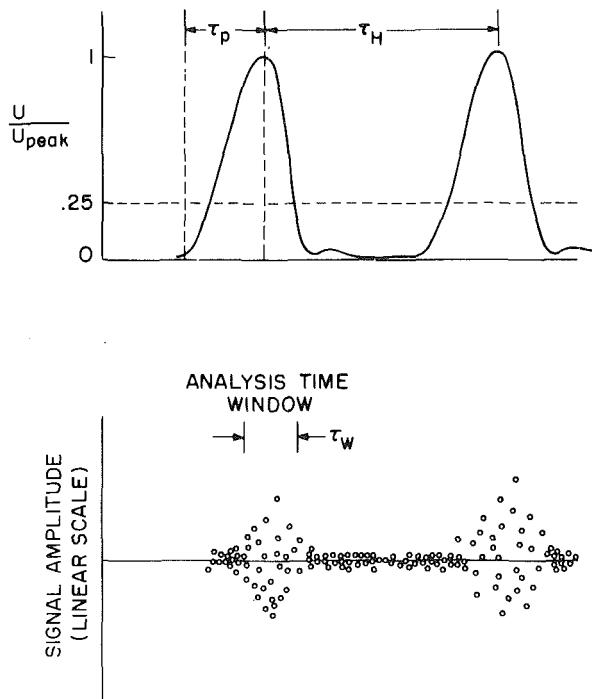$\omega$ = characteristic angular frequency, $2\pi/\tau_H$

**Fig. 3 Pulsatile waveform shape (upper record) and digitized wall pressure signal (lower record)—only every sixth digitized point is shown**

cross section (Fig. 2) with a minimum diameter, $d$, and expanding proximally and distally to intersect lengths of straight tubing on either end. Although constrictions of various shapes could be interchanged, all data reported here are for a single constriction with $(d/D) = 0.423$, i.e., an 82 percent area reduction. Preliminary tests demonstrated no essential differences in unsteady effects with several axisymmetric configurations. Experiments were conducted at pulsation frequencies of 1/2 Hz, 1 Hz, and 2 Hz, as well as for steady flow.

The pressure transducer[2] [31] had a sensing port 0.025 cm in diameter and was mounted flush with the inner wall of the distal tube. Axial variations of wall pressure fluctuations were obtained by moving the constriction relative to the stationary transducer. Willmarth and Roos [35] have shown that measurements of turbulent pressure fluctuations as made in these experiments will not be subject to large error if the highest frequency of interest is less than $U/d_t$, where $U$ is the characteristic convection speed and $d_t$ is the diameter of the active sensing area of the transducer. In these experiments $U/d_t \approx 20$ kHz, while the highest wall pressure fluctuation frequency component of interest was 2 kHz. No correction for transducer size was therefore required. The electrical signal from the piezoelectric sensing element was preamplified and high-pass filtered using a Princeton Applied Research Model 113 preamplifier, and recorded on a Tandberg 3000X AM tape recorder. Data tapes were analyzed at Massachusetts General Hospital on a computer system which was developed for clinical phonoangiography [9, 31, 32].

Data from the AM tapes were digitized using an Analogic AN5800 A/D converter with a 2000-Hz sampling rate, satisfying the Nyquist sampling theorem for frequencies up to 1000 Hz. The digitized bruits were then displayed on a Tektronix 4010 Graphics Terminal, and bruit sections were selected for

study. A time window of 0.128 s was centered over each bruit peak and the points within these windows were analyzed and averaged. Bruit peaks corresponded to periods of peak flow in the fluid system. The changes in flow velocity which occurred during the window time did not prove to be important; a maximum flow variation of $\pm 14.5$ percent was present in the 2 Hz pulsation experiments, with flow variations of $\pm 3.8$ percent for the 1 Hz runs and 1.0 percent for those at 1/2 Hz. Fig. 3 illustrates a sample waveform and digitized bruit with the time windows for spectral analysis denoted by vertical lines.

Each sement of digitized data selected for study was modified using a "Hanning" window, which provides for a cosine entry to and exit from the data segment, precluding the possibility of superimposing artifactual high-frequency information because of an instantaneous step.

By using a similar time window and averaging technique, spectra of the "diastolic" noise between bruits were also obtained, then subtracted from the spectra obtained at bruit peaks. Further details concerning the use of the phonoangiography analysis package and the digital signal processing which was used can be found elsewhere [9, 29, 31, 32].

The velocity waveform we used, Fig. 3($a$), is typical of that observed in human arterial flow. The velocity waveform was chosen to be intermediate to the aortic and femoral waveforms given by McDonald [35], Figs. 6.8 and 6.12$a$. The modulation parameter, $\beta$, was varied independently of the waveform shape; setting $\beta$ equal to unity produced a steady flow. In Fig. 3($b$), is a typical record of the transducer signal after digitization and storage in the computer. (For purposes of clarity, only every sixth stored point is displayed.) Fig. 4 presents a typical logarithmic display of rms pressure fluctuation amplitude per unit frequency interval as a function of frequency as computed using fast Fourier transform techniques [31, 32].

## Results and Discussion

The parameters which are important in the modeling of blood flow in the arteries include [33] the fluid kinematic viscosity, the arterial diameter, the flow velocity, the pulsation frequency, the depth of modulation of the velocity, and the fraction of
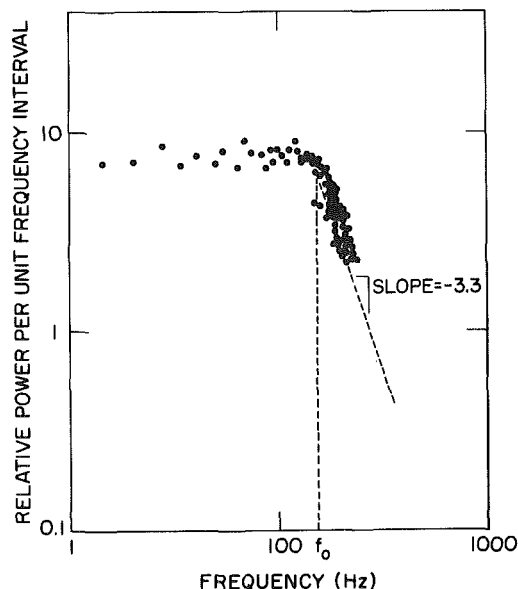


**Fig. 4 Power spectral density of wall pressure fluctuation spectrum. The frequency $f_o$ and high-frequency slope are noted. (These data are typical of steady-flow experiments using 100 cs fluid velocity $U = 100$ cm/s, $D = 1.59$ cm, $d = 0.675$ cm.)**

---

[2]The pressure transducer was obtained from Bolt, Beranek, and Newman, Cambridge, Mass. Transducer sensitivity was 1.88 $\mu V/\mu b$, and the frequency response was flat to within $\pm \frac{1}{2}$ dB from 20 Hz to 500 Hz.

the period comprising systole. These parameters can be arranged in the form of dimensionless groups which are employed in calculating simulation parameters. For example, the Reynolds number, $UD/\nu$, indicates the relative importance of fluid inertial forces and fluid viscous forces, while the Womersley parameter, $D(\omega/4\nu)^{1/2}$, characterizes the unsteady acceleration of the fluid. The dominant frequency component of the systolic portion of the flow pulse will appear greater than the characteristic heart frequency by the fraction $1/\gamma = \tau_{\text{heart}}/\tau_{\text{pulse}}$, as defined in Fig. 3.

For the purposes of comparing the effects of unsteady forces to those arising from inertia and viscosity, two dimensionless parameters are utilized. The first, $\Pi_1$, compares the unsteady acceleration, $du_j/dt$, to the convective acceleration, $u_j^2/l$, where $l$ is the characteristic axial distance between the point of minimum cross section and the point of reattachment of the turbulent jet distal to the constriction. The length, $l$, is a function of Reynolds number and we have used the values measured Back and Roshke [15]. Over this length, the velocity decreases from $u_j$ to $U$, the area-weighted mean arterial velocity in the unoccluded section of the artery. Conservation of mass requires $(u_j/U)$ to be equal to the area ratio, $A$, of the constriction where $A = D^2/d^2$. Then

$$\Pi_1 = \frac{(du_j/dt)}{(u_j^2/l)} = \frac{l(dU/dt)}{AU^2}$$

The magnitude of $(dU/dt)$ is characterized by the difference between peak systolic velocity and the time-mean velocity, $U_{\text{peak}} - U_{\text{mean}}$, divided by the rise of the systolic pulse, $\tau_p = \gamma \tau_H$. Using the modulation parameter $\beta \equiv U_{\text{mean}}/U_{\text{peak}}$, $\Pi_1$ is written

$$\Pi_1 = \left(\frac{\beta(1-\beta)}{A\gamma}\right) \left(\frac{l}{U_{\text{mean}}\tau_H}\right) \tag{1}$$

This parameter is essentially a modified Strouhal number.

The second nondimensional parameter compares the unsteady acceleration, $du_j/dt$, to a quantity characteristic of the viscous forces acting on the jet, $\nu u_j/d^2$:

$$\Pi_2 = \frac{(du_j/dt)}{(\nu u_j/d^2)}$$

In terms of the parameters $\beta$ and $\gamma$, this may be expressed as

$$\Pi_2 = \frac{(1-\beta)d^2}{\gamma \tau_H \nu}$$

Rewriting this result in terms of the heart frequency $\omega \equiv (2\pi/\tau_H)$ and the Womersley parameter $\alpha \equiv D(\omega/4\nu)^{1/2}$, we have

$$\Pi_2 = \frac{2(1-\beta)\alpha^2}{A\pi\gamma} \tag{2}$$

Typical physiological values of $\Pi_1$ range from 0.03–0.1, while values of $\Pi_2$ lie between 5 and 20.

Previous clinical [7, 9, 29] and in-vitro [19] studies have demonstrated that the two most significant parameters characterizing post-stenotic wall pressure fluctuation spectra are the break frequency, $f_o$, beyond which the spectral intensity falls sharply, and the logarithmic slope of the intensity beyond $f_o$. These quantities are illustrated in Fig. 4.

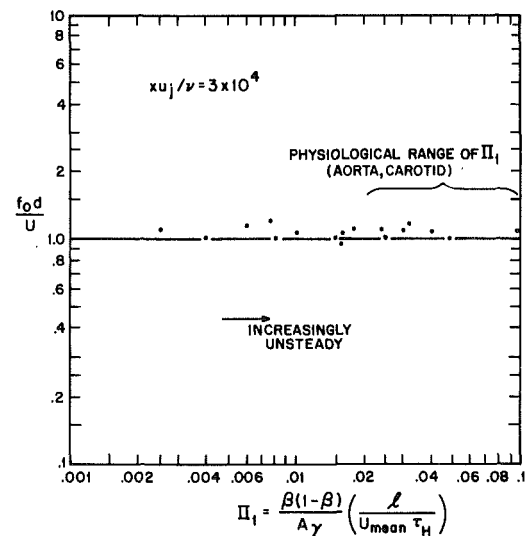Fig. 5 summarizes the measurements of $f_o$ obtained at peak



Fig. 6 Variation of the nondimensional break frequency ($f_o d/U$) with the parameter $\Pi_1$ (unsteady acceleration/convective acceleration)



Fig. 5 The value of $U/d$ versus break frequency at maximum systolic velocity found in pulsatile flow. Typical physiological values are shown only as a guide; all results plotted are experimental.
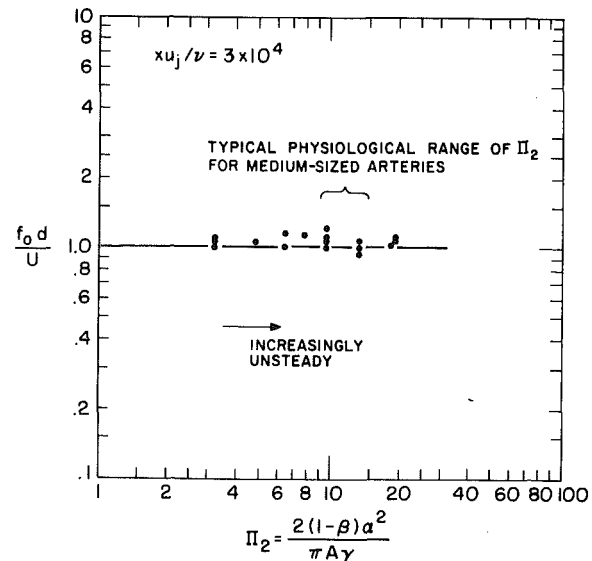


Fig. 7 Variation of the nondimensional break frequency ($f_o d/U$) with the parameter $\Pi_2$ (unsteady acceleration/viscous forces)

systole for various values of $\alpha$, $\beta$, $\tau_H$, and jet Reynolds number $Re_j \equiv (u_j d/\nu)$, where $u_j$ is the temporal peak of the volumetric mean jet velocity. A single physiological waveform (Fig. 3(a)) with $\gamma = 0.25$ was used for all tests. The spectra were obtained at the axial station exhibiting peak rms pressure fluctuation amplitude. Each point was obtained by averaging the spectra from 5–15 peak systolic time intervals. The value of $U$ assigned to each spectrum was the maximum value of velocity during the analysis interval.

The data are well correlated ($\pm 10$ percent) by the empirical steady-flow relation obtained by Fredberg [19] $(f_o d/U) = 1$. Physically, $U/d$ is an important frequency, as it is expected that the turbulent eddy size will scale roughly with $d$, while the speed at which these eddies are carried past the point of observation will approximate $U$. No systematic departures from this relation are apparent over the ranges $1/4 \leq \beta \leq 1$ and $0 \leq \alpha \leq 8$. This is more clearly illustrated in Figs. 6 and 7, where $f_o d/U$ is shown as a function of the unsteady parameters $\Pi_1$ and $\Pi_2$. $\Pi_1$ was varied by adjusting values of $\beta$ and $U_{\text{mean}}$, while $\Pi_2$ was allowed to range from 3 to 20. $\Pi_2$ was varied by adjusting $\beta$ and $\alpha$ while $\Pi_1$ was allowed to range from 0.002 to 0.1. The distance, $x$, distal to the minimum cross section at which the maximum turbulent wall pressure fluctuation intensity was found, was given by the relation $(x\,u_j/\nu) = 3 \times 10^4$, a correlation identical to that found by Fredberg [19] for steady flow. He demonstrated that the correlation of maximum intensity location, $(x\,u_j/\nu) = 3 \times 10^4$, did not change with the degree of constriction. These results imply that once some of the jet kinetic energy is converted to turbulent motion, the redistribution and subsequent decay of this turbulent energy are not affected by the walls; eddy-eddy interactions, rather than eddy wall interactions, govern the decay process.

Additional steady-flow data were obtained regarding the variation of $f_o$ proximal and distal to the point of maximum intensity. These data are given in Fig. 8. The 35 points at $(x\,u_j/\nu) = 3 \times 10^4$ include the unsteady data of Fig. 5. Because the intensity falls rapidly on either side of the maximum, it was necessary to take additional time segments to reduce
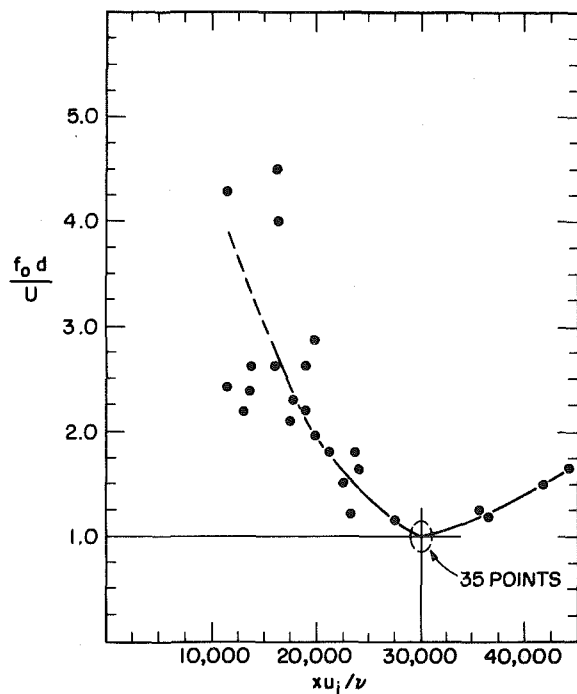
statistical fluctuations. The results suggest that $f_o$ increases distally and proximally from the maximum intensity point. Below $(x\,u_j/\nu) = 1.5 \times 10^4$, the intensity is so low that the results are subject to large uncertainties. Tobin, et al. [20] found that the value of $f_o$ decreased monotonically with distance distal to the maximum intensity point, although the observed decrease was not large.

The power spectral density of wall pressure fluctuations falls off sharply at high frequencies because of the continual transfer of energy from larger to smaller turbulent eddies. The physical process is analogous to that in turbulent pipe flow [33], although in the case of stenosed arteries the source of turbulent energy is localized in the jet emanating from the constriction and the intensity decays distal to the reattachment point. We have measured the logarithmic slope (see Fig. 4) of the pressure fluctuation spectra at peak intensity in unsteady flow, and both proximal and distal to the point of maximum intensity in steady flow. These data are given in Fig. 9. Clark [21] observed that the spectra of velocity fluctuations along the tube axis changed downstream of the point of maximum intensity. In his experiments, which were conducted at Reynolds numbers $800 \leq (UD/\nu) \leq 9000$, the spectrum slope decreased distally and an increasing amount of energy appeared in the low frequencies characteristic of turbulent pipe flow. In the Reynolds number range which we have investigated, the tube flow is laminar in the absence of a constriction.

The 35 points of $(x\,u_j/\nu) = 3 \times 10^4$ include all the unsteady conditions listed in Fig. 5. No differences of slope are apparent between peak systolic pulsatile flow and steady flow at the same velocity, at least for the physiological range simulated in these experiments. We also found that the absolute intensity of the turbulent pressure fluctuations at the distal point corresponding to maximum intensity was the same for the steady and unsteady experiments within the experimental reproducibility ($\pm 25$ percent) of this measurement.

The variation of rms wall pressure fluctuation intensity [19] with distance is also illustrated in Fig. 9. In clinical measurements of the bruit spectra produced by turbulence, it is reasonable to expect that both the break frequency and slope would be modified by transmission of the wall disturbances through the skin to the point of measurement and by signals arising from different points along the artery wall. This is illustrated
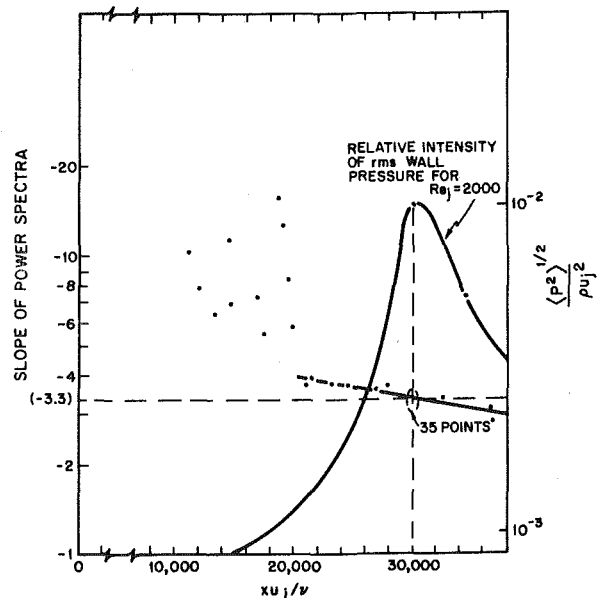


**Fig. 8 Variation of the nondimensional break frequency with distance distal to the stenosis**



**Fig. 9 Variation of spectral slope with distance distal to the stenosis—the rms wall pressure data are from Fredberg [19]**
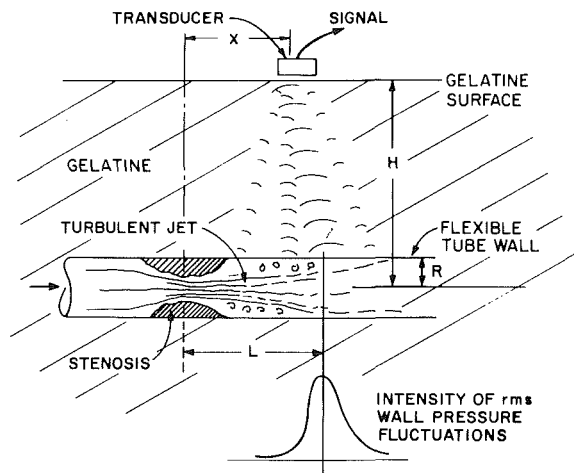
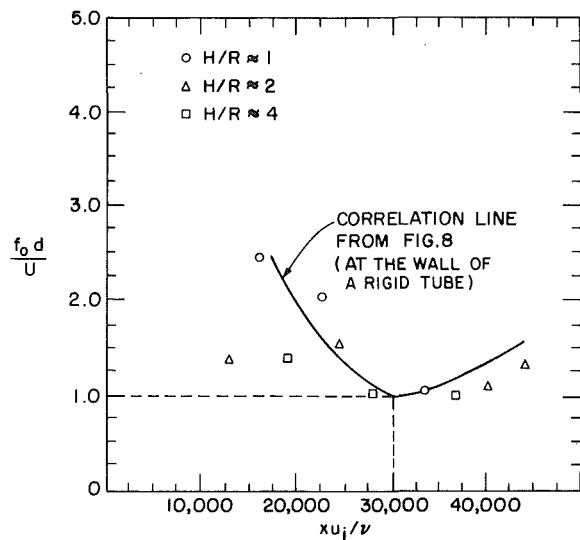**Fig. 10 Integration of wall pressure fluctuations at the gelatine surface**



**Fig. 11 Variation of break frequency measured with a microphone as a function of microphone location (x) distal to a stenosis for elastic tubing at various depths below the surface of a gelatine medium**

A final point of discussion concerns the method of spectral averaging and the choice of the characteristic velocity, $U$, to be the maximum value occurring during the systolic interval. It has been shown previously [7] that the rms intensity per unit frequency interval varies as $U^3$. Data obtained during any time interval will therefore be weighted heavily in favor of spectral characteristics pertaining to the maximum velocity. This is particularly true of high-frequency data, because $f_o \sim U$ and the spectra fall off rapidly beyond $f_o$. Increasing the temporal width of the analysis window would, nonetheless, tend to decrease the apparent value of $f_o d/U$, where $U$ is consistently taken to be the maximum during the analysis period.

The magnitude of this effect was evaluated in a cursory way by varying the analysis segment from 0.06 to 0.25 of the heart cycle time. The observed variation in $f_o$ was less than $\pm 10$ percent, which was within the overall experimental error for this parameter. Longer analysis times, e.g., unsampled or continuous analysis ($\tau_W/\tau_H = 1$), would yield lower values for the apparent break frequency and a distortion of the spectra from those reported here at peak systole. The magnitudes of these shifts and distortions are not known, but would probably depend intimately on the details of the pulsatile velocity waveform.

## Conclusions

One of the basic assumptions which has been adopted in interpreting clinical bruit spectra (phonoangiography) is that spectra obtained at the peak of systole are identical in all essential respects with spectra obtained in steady flow at the same velocity. The experiments reported here substantiate this assumption. For values of the nondimensional unsteady parameters $\Pi_1$ and $\Pi_2$ characteristic of medium-sized human arteries, no significant difference between the unsteady and steady values of $f_o$ or spectral slope were observed. Yellin and Peskin [18] and Clark [21] also concluded from other measurements that flow through an orifice at peak systole may be considered quasi-steady. There is probably good justification for the belief that waveform shape has only negligible influence upon the resulting turbulent spectra.

The present unsteady experiments as well as the analogous steady experiments of Fredberg [19] were conducted with smooth axisymmetric constrictions in rigid tubes. Other investigators, e.g., Fredberg [19], Tobin, et al. [20], Clark [21], and Sacks, et al. [28], have investigated different stenosis geometries or have obtained data in elastic tubes. Clark's results [21] demonstrate convincingly that the details of the stenosis geometry do not alter the turbulence spectrum significantly.

However, a less categorical statement is available with regard to the effects of wall properties. The preliminary results obtained at Vanderbilt University, Fig. 11, with an elastic tube imbedded in a gelatine medium suggest that, at least for the in-vivo situation where the artery is constrained by surrounding tissue, no resonant coupling exists between the wall motion and the high-frequency, small-scale turbulent spectra produced by a stenosis. The excellent correlation obtained by Duncan, et al. [9] between predicted residual lumen diameter ($d$) and x-ray angiographic measurements in stenosed human carotid arteries substantiates this conclusion. It is, however, worth noting that Gruber [29] obtained several isolated in-vivo spectra from stenosed external carotids in which distinct resonances were apparent. Perhaps under unusual circumstances, resonant interaction between the wall and the turbulent jet can occur.

An important practical conclusion derived from the present measurements is that the spectral break frequency, $f_o$, measured at the skin surface above a stenosed artery is relatively insensitive to position above the region of stenosis and to the width of the spectral interval taken at peak systole. Spatial sensitivity decreases with increasing skin depth between the artery and the transducer; for large values of $H/R$, the spectrum is

schematically in Fig. 10. Fredberg [8] has presented theoretical arguments which demonstrate that the slope of the spectrum is modified substantially by the addition of small-scale disturbances from different points along the artery wall. For large ratios of the artery depth below the skin, $H$, to tube radius, $R$, this result is equivalent to multiplying the rms spectra by a factor proportional to $1/f$. The break frequency $f_o$, however, would remain distinct. From Fig. 8 and the axial intensity distribution given in Fig. 9, one would expect the observed break frequency for $(H/R) >> 1$ to be slightly larger than the value observed at the wall at peak intensity.

Fig. 11 presents preliminary data obtained by one of us (WHP) on the break frequency as a function of artery depth. These steady flow simulation experiments were performed with the transducer placed on the surface of a gelatin medium surrounding an elastic tube. These results suggest that for values $(H/R) \leq 4$, the recorded break frequency at peak recorded intensity is equal within $\pm 20$ percent to that at the tube surface and increases slightly both proximally and distally. These results are consistent with the expectations generated by Figs. 8 and 9.

dominated by the wall pressure disturbances near the intensity maximum. Insensitivity to the width of the analysis time segment arises because the signal is dominated by events at peak systolic velocity; the rms wall pressure fluctuation intensity per unit frequency interval increases as $U^3$ for moderate Reynolds numbers characteristic of medium-sized human arteries.

Finally, we wish to emphasize that the observed break frequency for both unsteady and steady flow are correlated by the relation $f_o d/U \approx 1$. The velocity $U$ may be calculated easily if the flow rate, $Q$, and the distal diameter, $D$, are known. In interpreting in-vivo data, values of $U$ (or $D$ and $Q$) must be obtained. Gruber [29] has estimated $U$ from the absolute bruit intensity. Alternative methods of measuring $U$ (or $Q$ and $D$) directly would be most useful. Estimates of $D$ are subject to error if significant post-stenotic dilatation is present.

## Acknowledgment

## References

1 Fox, J. A., and Hugh, A. E., "Localization of Atheroma: A Theory Based on Boundary-Layer Separation," *British Heart Journal*, Vol. 28, 1966, pp. 388–398.

2 Duguid, J. B., "Mural Thrombosis in Arteries," *British Medical Bulletin*, Vol. 11, 1955, p. 36.

3 Gutstein, W. H., Lazzarini-Robertson, A., and La Taillade, J. N., "The role of Local Arterial Irritability in the Development of Arterio-Atherosclerosis," *American Journal of Pathology*, Vol. 42, 1963, p. 61.

4 Fry, D. L., "Responses of the Arterial Wall to Certain Physical Factors," *Atherosclerosis: Initiating Factors*, Ciba Foundation Symposium 12 (new series), Elsevier, Amsterdam, 1973, pp. 93–125.

5 Caro, C. G., Fitz-Gerald, J. M., and Schroter, R. C., "Atheroma and Wall Shear: Observation, Correlation and Proposal of a Shear Dependent Mass Transfer Mechanisms for Atherogenesis," *Proceedings of the Royal Society*, London (B), Vol. 177, 1971, pp. 109–159.

6 Stehbens, W. E., "The Role of Hemodynamics in the Pathogenesis of Atherosclerosis," *Progressive Cardiovascular Diseases*, Vol. 18, 1975, pp. 89–103.

7 Lees, R. S., and Dewey, C. F., Jr., "Phonoangiography: A New Noninvasive Diagnostic Method for Studying Arterial Disease," *Proceedings of the National Academy of Sciences*, Vol. 67, 1970, pp. 935–942.

8 Fredberg, J. J., "Pseudo-Sound Generation at Atherosclerotic Constrictions in Arteries," *Bulletin of Mathematical Biology*, Vol. 36, 1974, pp. 143–155.

9 Duncan, G. W., Gruber, J. O., Dewey, C. F., Jr., Myers, G. S., and Lees, R. S., "Evaluation of Carotid Stenosis by Phonoangiography," *New England Journal of Medicine*, Vol. 293, 1975, pp. 1124–1128.

10 Johansen, F. C., "Flow Through Pipe Orifices at Low Reynolds Numbers," *Proceedings of the Royal Society*, Vol. A126, 1929, pp. 231–245.

11 Forrester, J. H., and Young, D. F., "Flow Through a Converging-Diverging Tube and Its Implications in Occlusive Vascular Disease," *Journal of Biomechanics*, Vol. 3, 1970, pp. 297–316.

12 Young, D. F., and Tsai, F. Y., "Flow Characteristics in Models of Arterial Stenoses," *Journal of Biomechanics*, Vol. 6, 1973, pp. 395–410, 547–559.

13 Seeley, B. D., and Young, D. F., "Effect of Geometry on Pressure Losses Across Models of Arterial Stenoses," *Journal of Biomechanics*, Vol. 9, 1976, pp. 439–448.

14 Reul, H., Schoenmackers, J., and Starke, W., "Loss of Pressure, Energy, and Performance at Simulated Stenoses in Pulsatile Quasi-Physiological Flow," *Medical and Biological Engineering*, Vol. 10, 1972, pp. 711–718.

15 Back, L. H., and Roschke, E. J., "Shear-Layer Flow Regimes and Wave Instabilities and Reattachment Lengths Downstream of an Abrupt Circular Channel Expansion," *Journal of Applied Mechanics*, Vol. 39, 1972, pp. 677–681.

16 Roschke, E. J., and Back, L. H., "The Influence of Upstream Conditions on Flow Reattachment Lengths Downstream of an Abrupt Circular Channel Expansion," *Journal of Biomechanics*, Vol. 9, 1976, pp. 481–482.

17 Logan, S. E., "On the Fluid Mechanics of Human Coronary Artery Stenosis," *IEEE Trans. of Biomedical Engineering*, Vol. BME-22, 1975, pp. 327–334; Errata, pp. 454–455.

18 Yellin, E. L., and Peskin, C., "Large Amplitude Pulsatile Water Flow Across an Orifice," ASME Paper 73-WA/Bio-12, presented at the ASME Winter Annual Meeting, Detroit, November 11–15, 1973.

19 Fredberg, J. J., "Turbulent Pseudo-Sound Production in Atherosclerotic Arteries," PhD thesis, MIT, Cambridge, Mass., 1973; see also, "The Origin and Character of Vascular Murmurs," *Journal of Acoustical Society of America*, Vol. 61, 1977, pp. 1077–1085.

20 Tobin, R. J., Chang, I-Dee, and Koutsoyannis, S. P., "Wall Pressure and Displacements in a Simulation of Cardiovascular Murmur Generation," Stanford University Report SU DAAR No. 484, Jan. 1976; see also Tobin, R. J., and Chang, I-Dee, "Wall Pressure Scaling Downstream of Stenoses in Steady-Tube Flow," *Journal of Biomechanics*, Vol. 9, 1976, pp. 633–640.

21 Clark, C. "Turbulent Velocity Measurements in a Model of Aortic Stenosis," *Journal of Biomechanics*, Vol. 9, 1976, pp. 677–687.

22 Macagno, E. O., and Hung, T. K., "Computational and Experimental Study of a Captive Annular Eddy," *Journal of Fluid Mechanics*, Vol. 28, 1967, pp. 43–64.

23 Cheng, L. C., Robertson, J. M., and Clark, M. E., "Numerical Calculations of Plane Oscillatory Nonuniform Flow —II. Parametric Study of Pressure Gradient and Frequency With Square Wall Obstacles," *Journal of Biomechanics*, Vol. 6, 1973, pp. 521–538.

24 Daly, B. J., "A Numerical Study of Pulsatile Flow Through Stenosed Canine Femoral Arterise," *Journal of Biomechanics*, Vol. 9, 1976, pp. 465–475.

25 Fricke, F. R., "Pressure Fluctuations in Separated Flows," *Journal of Sound Vibrations*, Vol. 17, 1971, pp. 113–123.

26 Yellin, E. L., "Hydraulic Noise in Submerged and Bounded Liquid Jets," *Proceedings of Biomedical Fluid Mechanics Symposium*, ASME, N. Y., 1966, pp. 209–221.

27 Kim, B. M., and Corcoran, W. H., "Experimental Measurements of Turbulence Spectra Distal to Stenoses," Journal of Biomechanics, Vol. 7, 1974, pp. 335–342.

28 Sacks, A. H., Tickner, E. G., and Macdonald, I. B., "Criteria for the Onset of Vascular Murmurs," *Circular Restoration*, Vol. 24, 1971, pp. 249–256.

29 Gruber, J. O., "Clinical Applications of Phonoangiography," MS thesis, MIT, Cambridge, Mass., 1975.

30 Pitts, W. H., III, and Dewey, C. F., Jr., "Programmable Pulsatile Flow Apparatus for Simulation of Arterial Hemodynamics," *Proceedings of San Diego Biomedical Symposium*, Vol. 14, 1975, pp. 119–124.

31 Dewey, C. F., Jr., Metzinger, R. W., Klitzner, T. S., and Holford, S. K., "Analysis and Interpretation of Arterial Sounds Using a Small Clinical Computer System," *Proceedings of the San Diego Biomedical Symposium*, Vol. 12, 1973, pp. 119–130.

32 Dewey, C. F., Jr., Metzinger, R. W., and Lees, R. S., "A Small Replicable Computer System for Clinical Analysis," *Proceedings of the San Diego Biomedical Symposium*, Vol. 15, Academic Press, N. Y., 1976, pp. 41–50.

33 Clinch, J. M., "Measurements of the Wall Pressure Field at the Surface of a Smooth-Walled Pipe Containing Turbulent Water Flow," *Journal of Sound and Vibrations*, Vol. 9, 1969, pp. 398–418.

34 Willmarth, W. W., and Roos, R. W., "Resolution and Structure of the Wall Pressure Field Beneath a Turbulent Boundary Layer," *Journal of Fluid Mechanics*, Vol. 22, 1965, pp. 81–94.

35 McDonald, D. A., *Blood Flow in Arteries*, Williams and Wilkins Co., Baltimore, 2nd Edition, 1974, pp. 129 and 141.